AIAA JOURNAL
Vol. 31, No. 1, January 1993

Acoustic Radiation from a Thin Airfoil in Nonuniform Subsonic Flows

H. M. Atassi,* M. Dusey,† and C. M. Davis†
University of Notre Dame, Notre Dame, Indiana 46556

Noise resulting from the interaction of impinging unsteady vortical disturbances on a thin airfoil in subsonic flow is directly calculated using unsteady aerodynamic theory. Exact expressions for the far-field acoustic pressure, intensity, and total acoustic energy radiated are derived in terms of the Fourier transform of the unsteady pressure along the airfoil surface and account for both dipole and quadrupole effects. This paper provides benchmark results for the case of a thin airfoil for comparison with future calculations for a loaded airfoil. It is shown that the acoustic pressure pattern strongly depends on the value of the reduced frequency and the mean flow Mach number. The effects of an oblique gust are also examined and shown to significantly reduce the radiated acoustic power, which exhibits a maximum as the reduced frequency is increased. High frequency and noncompact source effects are also investigated and show multilobe directivity patterns that seem to recur at certain multiples of the reduced frequency.

Nomenclature

a = gust components, $\{a_1, a_2, a_3\}$
c_0 = speed of sound
D_I = acoustic directivity, Eq. (40)
D_p = pressure directivity, Eq. (39)
I = acoustic intensity
K = defined by Eq. (20)
K_1 = reduced frequency, Eq. (18)
k = gust wave numbers, $\{k_1, k_2, k_3\}$
M = Mach number
$\mathcal{P}$ = acoustic power
p = pressure
r = distance from airfoil center
t = time
u = unsteady velocity
x = physical coordinates, $\{x_1, x_2, x_3\}$
$\bar{x}$ = Prandtl-Glauert coordinates, $\{\bar{x}_1, \bar{x}_2, \bar{x}_3\}$
α = Fourier transform wave number, Eq. (31)
Λ = gust angle = $\tan^{-1}(k_3/k_1)$
θ = polar angle
ω = gust frequency

Subscripts

a = acoustic part of velocity
c = compact source approximation
0 = steady-state quantities
∞ = upstream conditions

Superscript

$'$ = time-dependent quantities

Introduction

WHEN a body moves in a nonuniform flow, sound is generated as a result of flow unsteadiness in the body frame of reference. This noise generation mechanism is common to aircraft and propulsive system structural components such as wings and propeller and turbomachine blades. These structures usually operate in nonuniform flows resulting from a variety of sources, such as atmospheric turbulence, inlet distortion, installation effects, blade tip vortices, and rotor-stator interaction. Thus, noise generated by this mechanism is often dubbed "interaction noise." Moreover, such noise tends to be loud and dominate other sources of noise.

Because of the motion of the body, flow nonuniformities are seen in the frame of reference of the body as convected vortical disturbances known as gusts.[1,2] The study of noise resulting from this mechanism is therefore closely related to the unsteady aerodynamics of vortical disturbances. The radiated sound is, in fact, the far field of such unsteady flows.

Unfortunately, it is difficult to find analytical solutions to unsteady compressible flows around bodies even for simple geometries. Thus, assuming an inviscid and non-heat-conducting fluid, the flow, for example, around a flat plate in a gust is obtained either by solving Possio's integral equation[3,4] or by a finite difference scheme.[5] Because of the widespread applications to unsteady airfoil theory, numerous asymptotic solutions were derived for the low frequency[6,7] and the high frequency[8,9,10] cases. With the exception of Ref. 10, these solutions focus on predicting the unsteady pressure distribution along the plate.

Amiet[11] gave an expression for the far-field acoustic power produced by an airfoil in subsonic turbulent flow. However, he assumes early on that the acoustic radiation of the airfoil can be determined by distributing dipoles over the airfoil surface equal in strength to the unsteady pressure jump along the surface. Thus, he accounts for only the dipole contribution to the far-field noise. The quadrupole effects of refraction due to the fluid motion as well as those of difraction by the leading and trailing edges of the airfoil are totally neglected. One of the objectives of the present paper is to examine these effects and to show that they can be significant at higher subsonic Mach number and higher frequencies.

For lifting airfoils in unsteady vortical flows, Goldstein and Atassi[12] and Atassi[13] developed a second-order theory for the limiting case of a vanishing Mach number and derived analytical formulas for the lift for two-dimensional gusts. Their results indicate significant effects of the mean flow on the gust response function. Myers and Kerschen[14] developed a high frequency subsonic model and calculated the far-field acoustic pressure in this limit. Scott and Atassi[15] and Scott[16] obtained numerical solutions for subsonic flows; these solutions give the airfoil surface unsteady pressure with high accuracy for three-dimensional gusts and for a broad range of reduced frequencies extending from 0 to 10.

Presented as Paper 90-3910 at the AIAA 13th Aeroacoustics Conference, Tallahassee, FL, Oct. 22-24, 1990; received May 13, 1991; revision received June 1, 1992; accepted for publication June 2, 1992.

*Professor, Department of Aerospace and Mechanical Engineering. Associate Fellow AIAA.
†Research Assistant, Department of Aerospace and Mechanical Engineering.

In this paper and in Ref. 17, the characteristics of the sound radiated from airfoils in subsonic flows and subject to three-dimensional gusts are investigated *directly* using a Possio's solver and the numerical solutions of Scott and Atassi.[5,15,16] The investigation will determine the effects of the mean flow Mach number, the airfoil geometry and mean flow incidence, and the upstream gust parameters on the far-field acoustic pressure, intensity, and total acoustic power radiated. It is important to note that the numerical solutions provide the flowfield in a finite domain surrounding the body. As a result, there are two methods for calculating the acoustic far field. First, we can still use Lighthill's[18] acoustic analogy to calculate the radiated sound from the dipole distribution along the body surface and the quadrupole distribution in the computation domain. Calculating the quadrupole contribution, however, necessitates the evaluation of volume integral. This leads to tedious calculations with dubious accuracy, particularly for lifting bodies at high speed where the mean flow around the body is quite complex. Note that the quadrupole contribution represents the effects of refraction and diffraction of the sound field as it propagates through the mean flow. At low subsonic speeds, these effects are often neglected. For unloaded blades, Hanson and Fink[19] have shown that for moderately subsonic speeds, the quadrupole contribution is negligible and that it is only significant at transonic speeds. However, for loaded blades, Goldstein et al.[20] have shown that the quadrupole contribution to the sound field is proportional to the mean flow circulation and will tend to become significant and comparable in magnitude to that of the dipole sound at higher Mach number and higher blade loading.

The second method for calculating the radiated sound is to directly use the flow quantities in the outer boundary of the computation domain to calculate the sound pressure and intensity. Unfortunately, computational solutions of unsteady flows, although yielding the surface pressure with high accuracy, do not have the far-field resolution to accurately describe the sound field. For example, the lift coefficient calculated by Scott and Atassi[15] is in excellent agreement with Atassi's[13] analytical solution for incompressible flow. However, Fig. 1 shows that the code gives inaccurate results for the computed far field pressure for a 3% thick airfoil in a transverse gust at a Mach number $M = 0.1$ and a reduced frequency $k_1 = 1.0$. This suggests that we use the computational results only in the near and middle fields where high accuracy is achieved. Kirchhoff's method is then used to calculate the acoustic far field from the midfield results. A similar approach was used by Farassat and Myers[21] and by George and Lyrintzis.[22]

The objective of this paper is to directly calculate the acoustic radiation of a thin airfoil in a nonuniform subsonic flow. For this case, semianalytical solutions can be obtained and will provide benchmark results for comparison with the more complex case of a highly loaded airfoil that will be investigated in the second paper.[17]

Aerodynamic Problem

Consider an unsteady three-dimensional weakly rotational flow $V(x, t)$ around a thin, flat-plate airfoil with chord length c, as shown in Fig. 2. The fluid is considered inviscid and non-heat conducting. We assume that the upstream flow mean velocity U_∞ is constant and that the airfoil is at zero angle of attack to U_∞. We further assume that the upstream rotational part of the flow is small and that the flow velocity, pressure, and density can be linearized about their mean values:

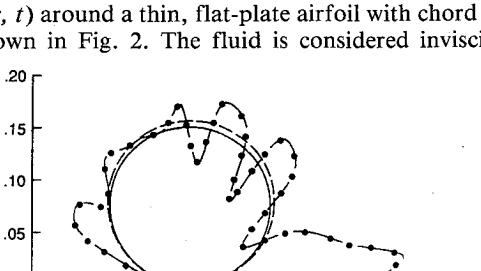

Fig. 1 Acoustic directivity for a 3% thick airfoil in a transverse gust at $M_\infty = 0.1$, $k_1 = 1.0$: — · —, direct calculation from Scott-Atassi's code; ——, Kirchhoff's method; ---, flat-plate semianalytical results.

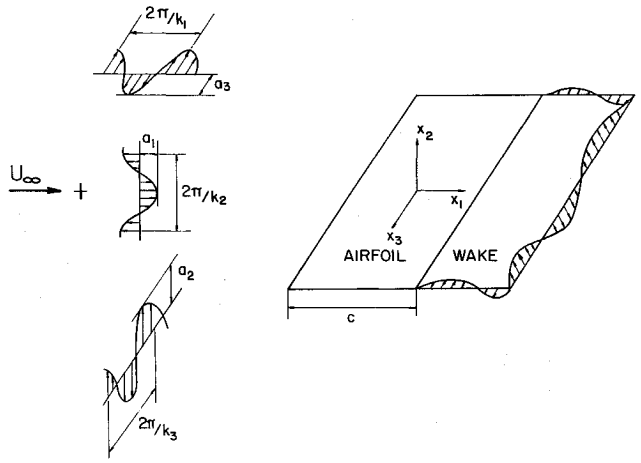

Fig. 2 Thin airfoil in a three-dimensional gust at subsonic speed.

$$V(x, t) = U_\infty + u(x, t) \tag{1}$$

$$p = p_0 + p'(x, t) \tag{2}$$

$$\rho = \rho_0 + \rho'(x, t) \tag{3}$$

If there are no upstream incident acoustic waves, the upstream flow can then be expressed as

$$V_\infty(x, t) = U_\infty i_1 + u_\infty(x - i_1 U_\infty t) \tag{4}$$

where u_∞ represents the upstream rotational disturbance of the flow, and we have taken the x_1 axis in the direction of U_∞ with unit vector i_1 and $U_\infty = |U_\infty|$. In this case it is shown in Refs. 2 and 23 that the total disturbance velocity can be split into a solenoidal but rotational part u_∞ convected by the mean flow and an acoustic potential part u_a:

$$u(x, t) = u_\infty(x - i_1 U_\infty t) + u_a(x, t) \tag{5}$$

where p' and ρ' are associated only with u_a and $p' = c_0^2 \rho'$.

Since the problem is linear, we break down u_∞ into its Fourier components and consider, without loss of generality, a single Fourier component. Thus, the upstream flow can be expressed as the real part of

$$V_\infty(x, t) = U_\infty i_1 + a e^{i(\omega t - k \cdot x)} \tag{6}$$

with the continuity equation

$$a \cdot k = 0 \tag{7}$$

where $a = \{a_1, a_2, a_3\}$ and $k = \{k_1, k_2, k_3\}$. If we normalize all lengths with respect to $c/2$ and all velocities with respect to U_∞, then $k_1 = \omega \cdot c/2U_\infty$ is referred to as the reduced frequency. The total velocity field can then be written as

$$V(x, t) = U_\infty i_1 + a e^{i(\omega t - k \cdot x)} + u_a(x, t) \tag{8}$$

The velocity $u_a(x, t) = \{u_{a1}, u_{a2}, u_{a3}\}$ is now the flow disturbance that results from the interaction of $a e^{i(\omega t - k \cdot x)}$ with the airfoil. Note that the far field of $u_a(x, t)$ represents the sound radiated from the airfoil.

The velocity $u_a(x, t)$ must satisfy the linearized Euler equations

$$\frac{D_0 \rho'}{Dt} + \nabla \cdot u_a = 0 \tag{9}$$

$$\rho_0 \frac{D_0 u_a}{Dt} = -\nabla p' \tag{10}$$

where

$$\frac{D_0}{Dt} = \frac{\partial}{\partial t} + U_\infty \frac{\partial}{\partial x_1}$$

and the boundary conditions

$$u_{a2}(x_1, 0, x_3) = -a_2 e^{i(\omega t - k\cdot x)} \quad \text{for} \quad -1 < x_1 < 1 \tag{11}$$

and p' and u_{a2} are continuous in the wake, $x_1 > 1$ and $x_2 = 0$. Taking the material derivative of Eq. (9) and subtracting from the divergence of Eq. (10) and using $p' = c_0^2 \rho'$, we get

$$\nabla^2 p' - \frac{1}{c_0^2} \frac{D_0^2}{Dt^2} p' = 0 \tag{12}$$

It is convenient to normalize p' and to factor out the dependence on t and x_3 by introducing

$$\tilde{p} = \frac{p'}{\rho_0 a_2 U_\infty} e^{-i(\omega t - k_3 x_3)} \tag{13}$$

Equation (12) can now be simplified by introducing the Prandtl-Glauert coordinates $\tilde{x} = \{\tilde{x}_1, \tilde{x}_2, \tilde{x}_3\}$, where

$$\tilde{x}_1 = x_1 \tag{14}$$

$$\tilde{x}_2 = \beta_\infty x_2 \tag{15}$$

$$\tilde{x}_3 = x_3 \tag{16}$$

where $\beta_\infty = \sqrt{1 - M_\infty^2}$. Finally, following Reissner[24] and Graham,[25] we introduce the following transformation:

$$\tilde{p} = P e^{iM_\infty K_1 \tilde{x}_1} \tag{17}$$

where

$$K_1 = \frac{k_1 M_\infty}{\beta_\infty^2} \tag{18}$$

Substituting Eqs. (13–17) into Eq. (12), we arrive at

$$(\tilde{\nabla}^2 + K^2) P = 0 \tag{19}$$

where

$$K = \sqrt{\frac{k_1^2 M_\infty^2}{\beta_\infty^4} - \frac{k_3^2}{\beta_\infty^2}} \tag{20}$$

and $\tilde{\nabla}$ is the del operator in the Prandtl-Glauert coordinates. Because the boundary condition (11) is not explicitly given in terms of P, the boundary-value problem is transformed into a singular integral equation known as Possio's equation.[3] This equation is usually solved by direct collocation and the numerical results provide the unsteady pressure along the plate surface.

Alternatively, we note that, if we introduce the velocity potential ϕ [i.e., $u_a = \nabla\phi$], it is easy to show that ϕ also satisfies the linear convective wave equation (12). Therefore, following steps (13–17), we introduce

$$\Phi = (\phi/a_2) \exp[-i(\omega t + iM_\infty K_1 \tilde{x}_1 - k_3 \tilde{x}_3)] \tag{21}$$

and we arrive at

$$(\tilde{\nabla}^2 + K^2)\Phi = 0 \tag{22}$$

with the boundary conditions

$$\frac{\partial \Phi}{\partial \tilde{x}_2} = -\frac{1}{\beta} e^{-i(k_1/\beta^2)\tilde{x}_1} \quad \text{for} \quad -1 < \tilde{x}_1 < 1 \tag{23}$$

$$\Delta\Phi = (\Delta\Phi)_{te} e^{-i(k_1/\beta^2)\tilde{x}_1} \quad \text{for} \quad \tilde{x}_1 > 1 \tag{24}$$

where $\Delta\Phi$ represents the jump of Φ across the wakeline and the subscript *te* denotes conditions at the trailing edge. The latter equation results from the continuity of the pressure in the wake. The boundary-value problem defined by Eqs. (21–24) was solved numerically by Scott and Atassi.[5]

Acoustic Field

The far fields of u_a and p' represent the acoustic sound radiated from the plate. A Possio solver will provide only the pressure distribution along the plate, whereas the numerical solution of Scott and Atassi[5] will yield the velocity and pressure fields inside the computational domain that may extend several chord lengths from the plate. However, despite the high accuracy of Scott and Atassi's numerical solution in the near field and the robustness of their code, their numerical solution in the far field is not as accurate. This is mainly because the velocity and pressure vanish in the far field except in the wake area; thus, the acoustic quantities become small at large distances from the plate. In addition, these effects are compounded by the fact that, in order to calculate, for example, the acoustic pressure, it is necessary to derive the potential function ϕ. This results in significant inaccuracy, as shown in Fig. 1, particularly near the wake region where a strong velocity gradient exists.

These findings suggest that we use the highly accurate numerical solutions to obtain the pressure distribution along the plate and to develop a mathematical procedure to calculate the far-field acoustic quantities. Similar methods were used by Farassat and Myers[21] and George and Lyrintzis.[22] Thus, in the following we assume that the pressure distribution along the plate is known. Using Green's theorem, we can express P in terms of its value along the airfoil:

$$P(\tilde{x}) = \frac{1}{2\pi} \int_{-1}^{1} \left(\Delta P \frac{\partial G}{\partial \tilde{y}_2} - G \frac{\partial \Delta P}{\partial \tilde{y}_2} \right) d\tilde{y}_1 \tag{25}$$

where $\tilde{x}$ is the observation point and $\tilde{y}$ is the source point. The free space Green's function for Eq. (19) is

$$G(|\tilde{x} - \tilde{y}|) = -i(\pi/2) H_0^{(2)}(K|\tilde{x} - \tilde{y}|) \tag{26}$$

For a flat-plate airfoil, Eq. (10) shows that $\partial P/\partial \tilde{y}_2 = 0$. Substituting Eq. (26) into Eq. (25), we get

$$P(x) = \frac{-i}{4} K \tilde{x}_2 \int_{-1}^{1} \Delta P(\tilde{y}_1) \frac{H_1^{(2)}(K|\tilde{x} - \tilde{y}|)}{|\tilde{x} - \tilde{y}|} d\tilde{y}_1 \tag{27}$$

In the far field, $|\tilde{x}| \ll |\tilde{y}|$, the expression in Eq. (27) can then be expanded in inverse power of $|\tilde{x}|$. Carrying out this expansion and reverting to the physical variables x and y, we obtain the following expression for the acoustic pressure:

$$p'(r, \theta) = \frac{\beta K^{1/2}}{\sqrt{8\pi}} \frac{e^{i(\pi/4)}}{\sqrt{r}} \frac{\sin\theta}{(1 - M^2 \sin^2\theta)^{3/4}}$$

$$\times \exp\{-ir[K(1 - M^2\sin^2\theta)^{1/2} - MK_1 \cos\theta]\} \tilde{F}(\alpha) + \mathcal{O}(1/r^{3/2}) \tag{28}$$

where

$$\tilde{F}(\alpha) = \int_{-1}^{1} \Delta p'(y_1) e^{i\alpha y_1} dy_1 \tag{29}$$

is the Fourier transform of the pressure jump along the x_1 axis:

$$\Delta p'(y_1) = p'(y_1,0+) - p'(y_1,0-) \tag{30}$$

and

$$\alpha = K\frac{\cos\theta}{\sqrt{1-M^2\sin^2\theta}} - MK_1 \tag{31}$$

The rms pressure is then

$$(\overline{p'^2})^{1/2} = \frac{\beta K^{1/2}}{2\sqrt{8\pi}}\frac{1}{\sqrt{r}}\frac{\sin\theta}{(1-M^2\sin^2\theta)^{3/4}}\,|\tilde{F}(\alpha)| \tag{32}$$

where we have neglected terms of $\mathcal{O}(1/r^{3/2})$ and higher. The expressions for the far-field expansion of the velocity components can then be readily obtained by substituting Eq. (28) into Eq. (10) and integrating:

$$u_{a1} = M\frac{K\cos\theta - MK_1\sqrt{1-M^2\sin^2\theta}}{K_1\sqrt{1-M^2\sin^2\theta} - MK\cos\theta}\,p' \tag{33}$$

$$u_{a2} = \frac{\beta^2 MK\sin\theta}{K_1\sqrt{1-M^2\sin^2\theta} - MK\cos\theta}\,p' \tag{34}$$

$$u_{a3} = \frac{Mk_3\sqrt{1-M^2\sin^2\theta}}{K_1\sqrt{1-M^2\sin^2\theta} - MK\cos\theta}\,p' \tag{35}$$

Since only the potential part u_a of the unsteady velocity contributes to the acoustic far field, the leading term of the acoustic intensity is identical with that of on isentropic irrotational flow. For such flows, a conserved expression for the acoustic intensity can be derived (Goldstein,[23] p. 41, and Myers[26]) as

$$\boldsymbol{I} = (p' + \rho_0 U_\infty u_{a1})\left[(u_{a1} + \frac{\rho'}{\rho_0}U_\infty)\boldsymbol{i}_1 + u_{a2}\boldsymbol{i}_2 + u_{a3}\boldsymbol{i}_3\right] \tag{36}$$

Note that, although $\boldsymbol{I}$ is second order, it depends only on first order quantities. Substituting Eqs. (28) and (33-35) into Eq. (36) and averaging over a period, we obtain the following expression for the time average intensity:

$$\bar{I} = \frac{1}{16\pi}\frac{\beta^4 MK}{K_1 r}\frac{\sin^2\theta}{[\sqrt{1-M^2\sin^2\theta} - (K/K_1)M\cos\theta]^2} \times |\tilde{F}(\alpha)|^2\left[\frac{\beta^2 K u_r}{1-M^2\sin^2\theta} + \frac{k_3 i_3}{\sqrt{1-M^2\sin^2\theta}}\right] + \mathcal{O}\left(\frac{1}{r^2}\right) \tag{37}$$

where u_r is the unit position vector. The expression for the acoustic power per unit span through a cylindrical surface surrounding the airfoil can then be derived immediately:

$$\mathcal{P} = \frac{\beta^6 MK^2}{8\pi K_1}\int_0^\pi \frac{\sin^2\theta}{(\sqrt{1-M^2\sin^2\theta} - (K/K_1)M\cos\theta]^2} \times \frac{|\tilde{F}(\alpha)|^2}{(1-M^2\sin^2\theta)}\,d\theta \tag{38}$$

Results and Discussion

We now examine the effects of the mean flow Mach number and the gust wave numbers on the acoustic pressure, intensity, and power. For the intensity we consider only the radial component $\bar{I}_r$. The magnitude and directivity of the average acoustic quantities are better estimated if we eliminate the dependence on the distance and consider the directivity of the pressure and the intensity defined by

$$D_p(\theta, M, K, K_1) = \sqrt{r}\,|p'| \tag{39}$$

$$D_I(\theta, M, K, K_1) = r\bar{I}_r \tag{40}$$

Mach Number and Frequency Effects

Examination of Eqs. (28-38) shows that the parameter K_1 plays an important role in determining the directivity of p' and $\bar{I}_r$. For small values of K_1, $\tilde{F}(\alpha)$ tends toward the negative of the unsteady lift $L'(M, k_1)$. This is the so-called compact source approximation, where the airfoil acts as if it were reduced to a single force. The only change from the acoustic field of a simple dipole is the dependence on the quantity $(1-M^2\sin^2\theta)$.

For a two-dimensional gust, using Amiet's[7] low frequency approximation for the lift for $K_1 \ll 1$, simple expressions can be derived for the directivity of the pressure and the intensity, and the total acoustic power

$$|p'| = \sqrt{\frac{\pi}{2}}\frac{K_1^{1/2}|S(k_1/\beta^2)|}{\sqrt{r}}\frac{\sin\theta}{(1-M^2\sin^2\theta)^{3/4}} + \mathcal{O}(K_1) \tag{41}$$

$$\bar{I}_r = \frac{\pi}{4}\beta^4 K_1 M\,|S^2(k_1/\beta^2)|\,\frac{\sin^2\theta}{r(1-M^2\sin^2\theta)} \times \frac{1}{(\sqrt{1-M^2\sin^2\theta} - M\cos\theta)^2} + \mathcal{O}(K_1^{3/2}) \tag{42}$$

where $S(k_1) = L'(0, K_1)/2\pi$ is the Sears[27] function. Note that $|S(k_1)| \approx 1/\sqrt{1+2\pi k_1}$. This shows that at low frequency the effect of the mean flow Mach number is to deform the pattern of the acoustic pressure from a circle into a pearlike shape. For a small Mach number, we can further neglect terms of $\mathcal{O}(M^2)$, and integrate Eq. (42) to obtain the following simple expression for the total acoustic power radiated from the airfoil:

$$\mathcal{P} = \frac{\pi^2}{4}K_1 M\,|S^2(k_1)| + \mathcal{O}(K_1^{3/2}, M^2) \tag{43}$$

At a low Mach number and a relatively high reduced frequency k_1 but $K_1 \ll 1$, a case pertaining to marine propellers,[28] Eqs. (41-43) give good approximations for $|p'|$, $\bar{I}_r$, and $\mathcal{P}$. Thus, the magnitude of the acoustic pressure first increases with the reduced frequency k_1, and then it tends toward a limit as k_1 becomes large.

For moderate values of K_1, Fig. 3 shows that, at $K_1 = 1$, D_p is significantly increased at higher M, thus indicating strong Mach number effects. It is also interesting to note that the directivity is no longer symmetric but appears to have a slight tilt in the downstream direction. For K_1 larger than about $\pi/2$ (e.g., for $K_1 = 3.0$), Fig. 4 shows the appearance of lobes in the pressure directivity. These effects are the so-called noncompact sources effects. Figure 5 shows plots of D_p at $M = 0.8$ and various frequencies. As K_1 increases the magnitude of the acoustic pressure decreases while the number of

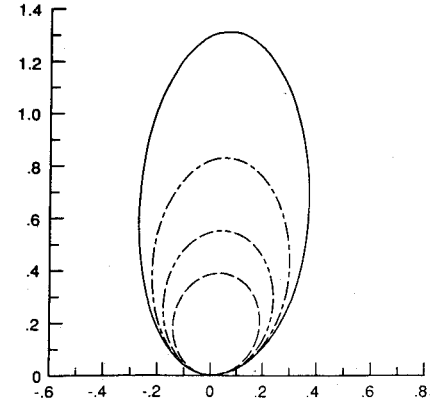

Fig. 3 Pressure directivity D_p for a flat plate in a transverse gust at $K_1 = 1.0$: ——, $k_1 = 0.25$, $M = 0.883$; — · —, $k_1 = 0.50$, $M = 0.781$; - · · -, $k_1 = 1.00$, $M = 0.618$; - - -, $k_1 = 2.00$, $M = 0.414$.

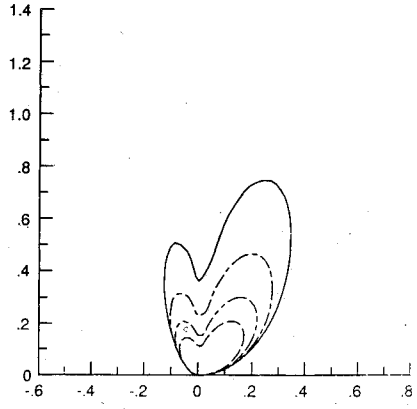

Fig. 4 Pressure directivity D_p for a flat plate in a transverse gust at $K_1 = 3.0$: ——, $k_1 = 0.75$, $M = 0.883$; — · —, $k_1 = 1.50$, $M = 0.781$; - · · -, $k_1 = 3.00$, $M = 0.618$; ---, $k_1 = 6.00$, $M = 0.414$.

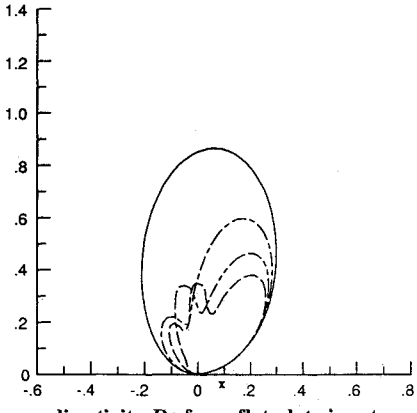

Fig. 5 Pressure directivity D_p for a flat plate in a transverse gust at $M = 0.8$: ——, $k_1 = 0.5$, $K_1 = 1.11$; — · —, $k_1 = 1.0$, $K_1 = 2.22$; - · · -, $k_1 = 1.5$, $K_1 = 3.34$; ---, $k_1 = 2.0$, $K_1 = 4.46$.

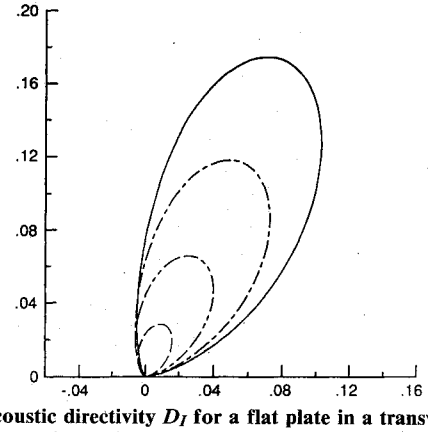

Fig. 6 Acoustic directivity D_I for a flat plate in a transverse gust at $K_1 = 1.0$: ——, $k_1 = 0.25$, $M = 0.883$; — · —, $k_1 = 0.50$, $M = 0.781$; - · · -, $k_1 = 1.00$, $M = 0.618$; ---, $k_1 = 2.00$, $M = 0.414$.

lobes increases. For large values of K_1, the maximum of D_p would occur at

$$\theta_{\max} = \sin^{-1}\left(\frac{1}{\sqrt{1+M^2}}\right) \tag{44}$$

Hence, as we approach sonic velocity, $\theta_{\max} \to 45$ deg.

Figures 6, 7, and 8 show polar plots of the directivity D_I for the same conditions as Figs. 3, 4, and 5, respectively. Comparing D_I with D_p, we note the increased tilt of the intensity plots in the downstream direction, indicating that most of the acoustic energy is radiated downstream. Thus, the lobes which appear in the pressure directivity plots are almost hidden by the fact that they occur mainly at $|\theta| > \pi/2$, where D_I is significantly reduced.

Oblique Gust Effects

We now consider the effects of a three-dimensional gust at an angle $\Lambda = \tan^{-1}(k_3/k_1)$. Figures 9–11 are plots of the pressure directivity and Figs. 12, 13, and 14 are plots of the acoustic intensity for the same condition as that in Figs. 3, 4, and 5, respectively, except that $\Lambda = 30$ deg. Note that when $K \leq 0$ there is no acoustic radiation. This cutoff condition is illustrated by comparing Figs. 3 and 9. There is no acoustic radiation for the case corresponding to $k_1 = 2.0$ and $M = 0.414$, because these conditions correspond to $K = -0.269$. It is also seen that the effect of k_3 is to reduce the magnitude of the pressure, but this effect strongly depends on how much k_3 reduces the value of K in comparison to K_1. When $K \approx K_1$, these effects become insignificant. However, the effects of the

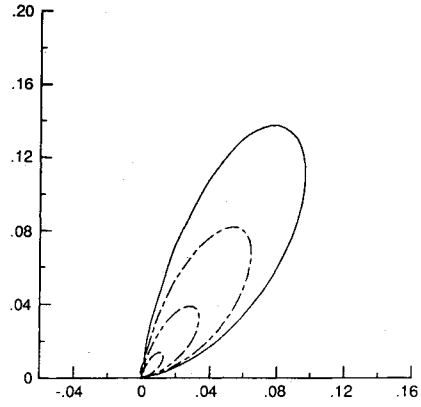

Fig. 7 Acoustic directivity D_I for a flat plate in a transverse gust at $K_1 = 3.0$: ——, $k_1 = 0.75$, $M = 0.883$; — · —, $k_1 = 1.50$, $M = 0.781$; - · · -, $k_1 = 3.00$, $M = 0.618$; ---, $k_1 = 6.00$, $M = 0.414$.

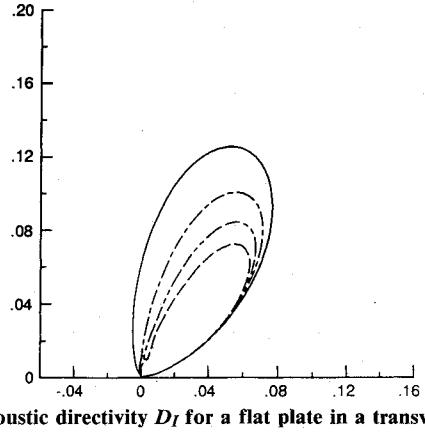

Fig. 8 Acoustic directivity D_I for a flat plate in a transverse gust at $M = 0.8$: ——, $k_1 = 0.5$, $K_1 = 1.11$; — · —, $k_1 = 1.0$, $K_1 = 2.22$; - · · -, $k_1 = 1.5$, $K_1 = 3.34$; ---, $k_1 = 2.0$, $K_1 = 4.46$.

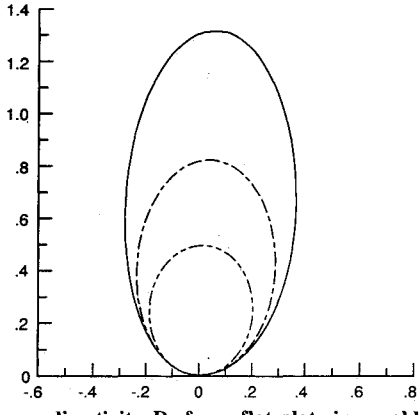

Fig. 9 Pressure directivity D_p for a flat plate in an oblique gust at $\Lambda = 30$ deg, $K_1 = 1.0$: ——, $k_1 = 0.25$, $M = 0.883$; — · —, $k_1 = 0.50$, $M = 0.781$; - · · -, $k_1 = 1.00$, $M = 0.618$.

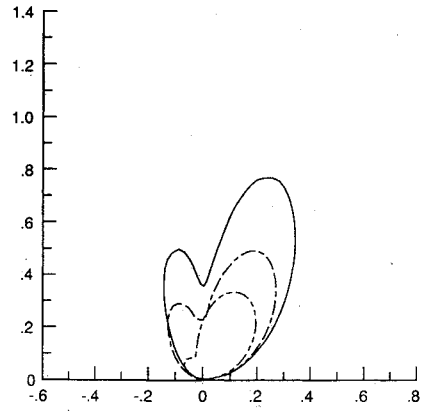

Fig. 10 Pressure directivity D_p for a flat plate in an oblique gust at $\Lambda = 30$ deg, $K_1 = 3.0$: ——, $k_1 = 0.75$, $M = 0.883$; — · —, $k_1 = 1.50$, $M = 0.781$; - ··· -, $k_1 = 3.00$, $M = 0.618$; ---, $k_1 = 6.00$, $M = 0.414$.

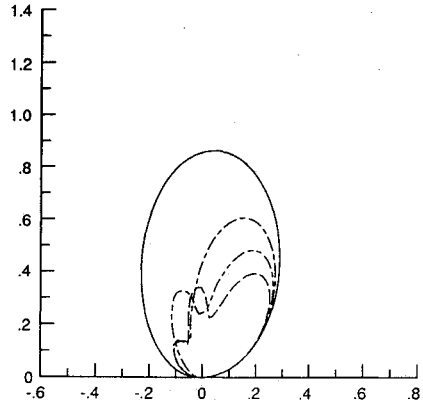

Fig. 11 Pressure directivity D_p for a flat plate in an oblique gust at $\Lambda = 30$ deg, $M = 0.8$: ——, $k_1 = 0.5$, $K_1 = 1.11$; — · —, $k_1 = 1.0$, $K_1 = 2.22$; - ··· -, $k_1 = 1.5$, $K_1 = 3.34$; ---, $k_1 = 2.0$, $K_1 = 4.46$.

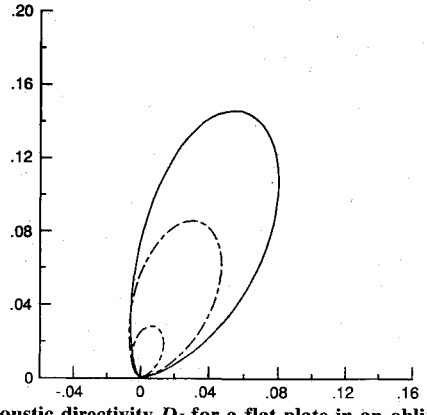

Fig. 12 Acoustic directivity D_I for a flat plate in an oblique gust at $\Lambda = 30$ deg, $K_1 = 1.0$: ——, $k_1 = 0.25$, $M = 0.883$; — · —, $k_1 = 0.50$, $M = 0.781$; - ··· -, $k_1 = 1.00$, $M = 0.618$.

gust obliqueness are much more significant on the acoustic intensity. They are, of course, particularly strong for $K \ll K_1$, as shown in Figs. 12–14.

Acoustic Power

In Fig. 15 we have plotted the total acoustic power resulting from a transverse gust vs the reduced frequency k_1 for different values of the Mach number. At low M, $\mathcal{P}$ tends to a limit as long as K_1 is of order unity. At larger M, $\mathcal{P}$ first increases as k_1 increases, reaches a maximum at k_{1m}, and then decreases. Note that k_{1m} also decreases with increasing M. These results indicate that it is possible to significantly reduce the acoustic power by avoiding disturbances of frequencies in certain range. Figure 16 is a plot of $\mathcal{P}$ vs k_1 for an oblique gust at $\Lambda = 30$ deg at two values of M, 0.6 and 0.8. Note the

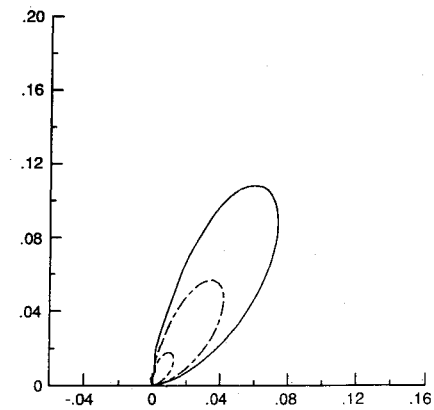

Fig. 13 Acoustic directivity D_I for a flat plate in an oblique gust at $\Lambda = 30$ deg, $K_1 = 3.0$: ——, $k_1 = 0.75$, $M = 0.883$; — · —, $k_1 = 1.50$, $M = 0.781$; - ··· -, $k_1 = 3.00$, $M = 0.618$; ---, $k_1 = 6.00$, $M = 0.414$.

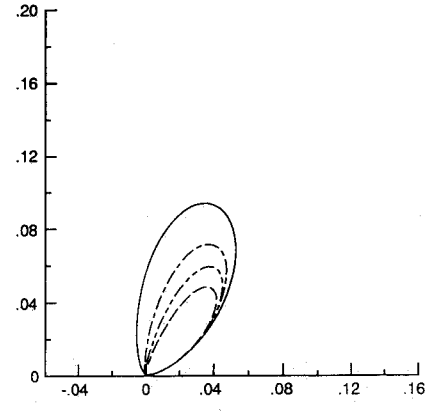

Fig. 14 Acoustic directivity D_I for a flat plate in an oblique gust at $\Lambda = 30$ deg, $M = 0.8$: ——, $k_1 = 0.5$, $K_1 = 1.11$; — · —, $k_1 = 1.0$, $K_1 = 2.22$; - ··· -, $k_1 = 1.5$, $K_1 = 3.34$; ---, $k_1 = 2.0$, $K_1 = 4.46$.

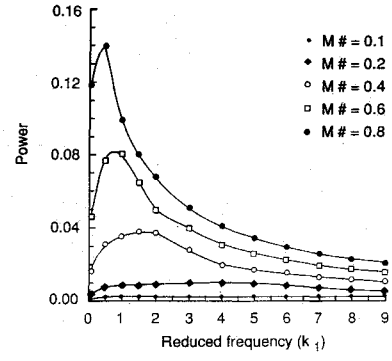

Fig. 15 Acoustic power radiated from a flat plate in a transverse gust vs the reduced frequency at various Mach numbers.

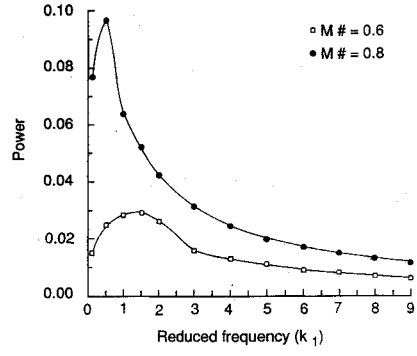

Fig. 16 Acoustic power radiated from a flat plate in an oblique gust vs the reduced frequency at various Mach numbers ($\Lambda = 30$ deg).

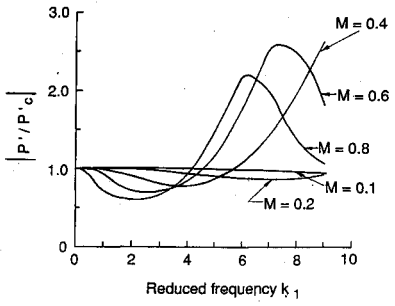

Fig. 17 Ratio of acoustic power to compact source calculated power for a flat plate in a transverse gust vs k_1 at various Mach numbers.

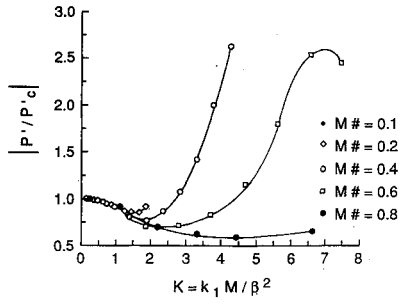

Fig. 18 Ratio of acoustic power to compact source calculated power for a flat plate in a transverse gust vs K_1 at various Mach numbers.

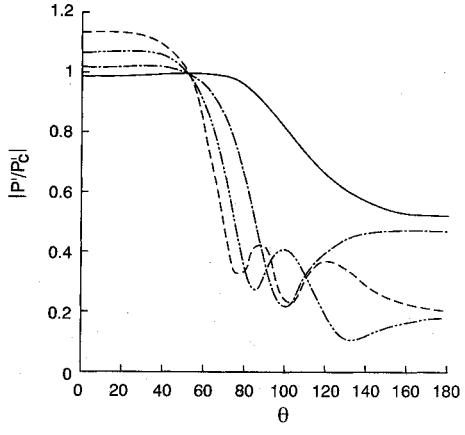

Fig. 19 Ratio of acoustic pressure to compact source pressure vs θ: ——, $k_1 = 0.5$; — · —, $k_1 = 1.0$; - · · -, $k_1 = 1.5$; ---, $k_1 = 2.00$.

significant reduction of the acoustic power particularly at low and moderate frequencies.

High Frequency and Noncompact Source Effects

Finally, we examine high frequency effects on the acoustic power by comparison with the commonly used compact source approximation. We have plotted in Fig. 17 the ratio $\mathcal{P}/\mathcal{P}_c$, where $\mathcal{P}_c$ is the acoustic power calculated using the compact source approximation (i.e., $\alpha_0 = 0$) in Eq. (31), vs k_1 for various M. The results exhibit large variations as k_1 and M increase. However, when $\mathcal{P}/\mathcal{P}_c$ is plotted vs K_1 in Fig. 18, the results are reduced to a single curve for $K_1 < \pi/2$. On the other hand, for larger values of K_1 the results are scattered indicating a strong dependence on M. The compact source approximation is definitely not valid at large K_1. However, it is significant to note that the ratio can vary from 0.5 to 2.5; thus, for certain values of k_1 and M, $\mathcal{P}/\mathcal{P}_c$ can be larger than unity. To explain how this ratio can become larger than unity, we have plotted in Figs. 19 and 20 the ratio $\tilde{F}(\alpha)/\tilde{F}(0)$ vs the direction angle θ at M = 0.8 and various values of k_1. This ratio is equal to the ratio of the far-field acoustic pressures p'/p'_c. These figures clearly show that at moderate and high frequencies the sound radiated in the downstream direction is

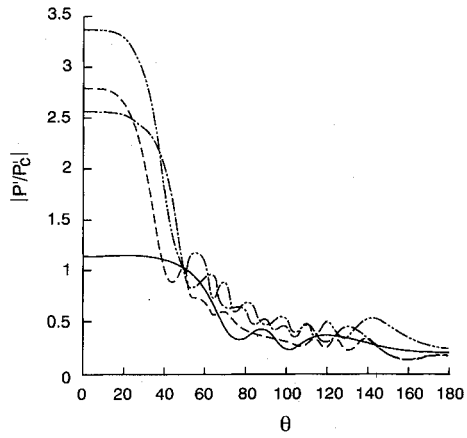

Fig. 20 Ratio of acoustic pressure to compact source pressure vs θ: ——, $k_1 = 2.0$; — · —, $k_1 = 5.0$; - · · -, $k_1 = 7.0$; ---, $k_1 = 10.0$.

enhanced (ratio above unity) by the distribution of the dipoles along the airfoil surface, which affects their phase, whereas the sound radiated upstream is significantly reduced. Moreover, this effect is stronger at high frequencies and help explain the strong downstream directionality of the radiated sound.

Conclusions

The sound resulting from the interaction of a three-dimensional gust with an airfoil is calculated *directly* using the midfield results of unsteady aerodynamic codes on a Kirchhoff surface. This approach avoids the difficulties associated with the loss of accuracy in the outer computational domain. The current paper provides benchmark results for the case of a flat plate airfoil for comparison with the more complex case of a loaded airfoil, which is given in another paper.[17] The results of the current study can be summarized as follows.

The acoustic pressure and directivity strongly depend on the frequency K_1, which is approximately equal to π times the ratio of the airfoil chord to an average upstream-downstream wavelength $\bar{\lambda}$[7]. When $c < \bar{\lambda}/2$, the pressure directivity is smooth. However, when $c > \bar{\lambda}/2$, lobes appear, indicating strong directional patterns.

For a gust propagating at an angle Λ to the airfoil chord, the acoustic pressure is generally less than that for a purely transverse gust. The reduction in the acoustic pressure is very significant when $K \ll K_1$, but it is insignificant when $K \approx K_1$. Of course, when $K \leq 0$, there is no sound radiated. The effects of an oblique gust are more significant on the acoustic intensity than on the acoustic pressure.

The acoustic power for moderate and high values of the mean flow Mach number M exhibits a maximum as the reduced frequency k_1 increases. This behavior can be used for noise reduction by avoiding frequencies where $\mathcal{P}$ is large. The obliqueness of the gust produces a significant reduction in the acoustic power, particularly at low and moderate frequencies.

Finally, an examination of the popular compact source approximation shows that it is adequate for $K_1 < \pi/2$. As K_1 becomes larger, this approximation could give much larger or much smaller values for the acoustic power, depending on the value of the mean flow Mach number.

Acknowledgments

This research was supported by NASA Lewis Research Center under Grant NAG-3732. The authors thank John F. Groeneweg for his support throughout this work.

References

[1]Kemp, N., and Sears, W. R., "The Unsteady Forces Due to Viscous Wakes in Turbomachines," *Journal of the Aeronautical Sciences*, Vol. 22, No. 7, 1955, pp. 478–483.

[2]Atassi, H. M., "Unsteady Vortical Disturbances Around Bodies," *Proceedings of the Tenth U.S. National Congress of Applied Mechan-*

ics, edited by J. P. Lamb, American Society of Mechanical Engineers, New York, 1986, pp. 475–484.

[3]Possio, C., "L'Azione Aerodinamica sul Profilo Oscillante in un Fluido Compressibile a Velocita Ipsonora," *L'Aerotecnica,* Vol. 18, No. 4, 1938, pp. 441–458.

[4]Graham, J. M. R., "Similarity Rules for Thin Airfoils in Non-Stationary Subsonic Flows," *Journal of Fluid Mechanics,* Vol. 43, Pt. 4, 1970, pp. 753–766.

[5]Scott, J. R., and Atassi, H. M., "Numerical Solution of Periodic Vortical Flows About a Thin Airfoil," AIAA Paper 89-1691, June 1989.

[6]Osborne, C., "Unsteady Thin-Airfoil Theory for Subsonic Flow," *AIAA Journal,* Vol. 11, No. 2, 1973, pp. 205–209.

[7]Amiet, R. K., "Compressibility Effects in Unsteady Thin-Airfoil Theory," *AIAA Journal,* Vol. 12, No. 2, 1974, pp. 253–255.

[8]Adamczyk, J. J., "The Passage of an Infinite Swept Airfoil Through an Oblique Gust," *Journal of Aircraft,* Vol. 11, No. 5, 1974, pp. 281–287.

[9]Amiet, R. K., "High Frequency Thin-Airfoil Theory for Subsonic Flow," *AIAA Journal,* Vol. 14, No. 8, 1976, pp. 1076–1082.

[10]Martinez, R., and Widnall, S. E., "Unified Aerodynamic-Acoustic Theory for a Thin Rectangular Wing Encountering a Gust," *AIAA Journal,* Vol. 18, 1980, pp. 636–645.

[11]Amiet, R. K., "Acoustic Radiation from an Airfoil in a Turbulent Stream," *Journal of Sound and Vibration,* Vol. 41, No. 4, 1976, pp. 407–420.

[12]Goldstein, M. E., and Atassi, H. M., "A Complete Second-Order Theory for the Unsteady Flow About an Airfoil Due to a Periodic Gust," *Journal of Fluid Mechanics,* Vol. 74, 1976, pp. 741–765.

[13]Atassi, H. M., "The Sears Problem for a Lifting Airfoil Revisited—New Results," *Journal of Fluid Mechanics,* Vol. 141, 1984, pp. 109–122.

[14]Myers, M. R., and Kerschen, E. J., "Effect of Airfoil Mean Loading on Convected Gust Interaction Noise," AIAA Paper 84-2324, Oct. 1984.

[15]Scott, J. R., and Atassi, H. M., "Numerical Solutions of the Linearized Euler Equations for Unsteady Vortical Flows Around Lifting Airfoils," AIAA Paper 90-0694, Jan. 1990.

[16]Scott, J. R., "Compressible Flows with Periodic Vortical Disturbances Around Lifting Airfoils," Ph.D. Dissertation, Univ. of Notre Dame, Notre Dame, IN, 1990.

[17]Atassi, H. M., Subramaniam, S., and Scott, J. R., "Acoustic Radiation From a Lifting Airfoil in Nonuniform Subsonic Flows," AIAA Paper 90-3911, Oct. 1990.

[18]Lighthill, J. M., "On Sound Generated Aerodynamically. I. General Theory," *Proceedings of the Royal Society of London, Series A,* Vol. 211A, 1952, pp. 564–587.

[19]Hanson, D. B., and Fink, M. R., "The Importance or Quadrupole Sources in Prediction of Transonic Tip Speed Propeller Noise," *Journal of Sound and Vibration,* Vol. 62, No. 1, 1979, pp. 19–38.

[20]Goldstein, M. E., Dittmar, J. H., and Gelder, T. F., "Combined Quadrupole-Dipole Model for Inlet Flow Distortion Noise," NASA TN D-7676, May 1974.

[21]Farassat, F., and Myers, M. K., "Extension of Kirchhoff's Formula to Radiation From Moving Surfaces," *Journal of Sound and Vibration,* Vol. 123, No. 3, 1988, pp. 451–460.

[22]George, A. R., and Lyrintzis, A. S., "Acoustics of Transonic Blade-Vortex Interactions," *AIAA Journal,* Vol. 26, No. 7, 1988, pp. 769–776.

[23]Goldstein, M. E., *Aeroacoustics,* McGraw-Hill, New York, 1976.

[24]Reissner, E., "On the Application of Mathieu Functions in the Theory of Subsonic Compressible Flow Past Oscillating Airfoils," NACA-TN 2363, 1951.

[25]Graham, J. M. R., "Lifting Surface Theory for the Problem of Arbitrarily Yawed Sinusoidal Gust Incident on a Thin Airfoil in Incompressible Flow," *Aeronautical Quarterly,* Vol. 21, No. 2, 1970, pp. 182–198.

[26]Myers, M. K., "Transport of Energy by Disturbances in Arbitrary Steady Flows," *Journal of Fluid Mechanics,* Vol. 226, 1991, pp. 383–400.

[27]Sears, W. R., "Some Aspects of Non-Stationary Airfoil Theory and Its Practical Application," *Journal of the Aeronautical Sciences,* Vol. 8, No. 3, 1941, pp. 104–108.

[28]Blake, W. K., "Aero-Hydroacoustics for Ships," David Taylor Naval Ship Research and Development Center, DTNSRDC Rept. 84/010, June 1984.